

# Discharge at / near the interface of two immiscible liquids and its application in nanomaterial synthesis

A. Hamdan<sup>1</sup>

<sup>1</sup> *Groupe de physique des plasmas, Département de Physique, Université de Montréal, 1375 Avenue Thérèse-Lavoie-Roux, Montréal, H2V 0B3, Québec, Canada*

**Abstract:** Discharge in liquid is used to synthesize nanomaterials by electrode erosion or by ion reduction. In this communication, we present a new type of in-liquid discharge that is at / near the interface of two immiscible liquids: a hydrocarbon liquid and an aqueous solution. The electrical and optical characteristics of the discharge are presented, and the nanomaterials produced under different conditions are characterized. The results demonstrate that various binary and ternary nanoalloys may be synthesized using the proposed setup.

**Keywords:** Discharge in liquid, immiscible liquids, nanomaterials.

## 1. Introduction

Plasma–liquid systems have shown great potential for use in the production of nanomaterials [1], among other applications [2]. Most interactions between the plasma and the liquid occur at the interface, and thus, it is considered the reaction zone. In this context, various plasma–liquid systems have been studied over the last two decades. These systems can be classified into four categories: i) plasma in a gas phase in contact with liquid, ii) plasma in liquid, iii) plasma in liquid with gaseous bubbles, and iv) plasma in a gas phase with liquid droplets [3].

In-liquid discharges produce nanomaterials via two major pathways: electrode erosion [1] and ion reduction [4]. The former is based on the interaction between the plasma and the electrode surface. The electrode material evaporates under the effect of local heat (thousands of Kelvin), and the evaporated material is introduced into the plasma channel, whose composition is strongly dependent on the utilized liquid [1]. The interactions between the evaporated material and the plasma species leads to the production of nanomaterial. Depending on the electrode and liquid compositions, various nanomaterials may be synthesized. In general, discharges between metal electrodes in water produce metal oxide nanoparticles such as CuO, Cu<sub>2</sub>O, NiO, CoO, Al<sub>2</sub>O<sub>3</sub>, etc. [1, 5, 6], while discharges between metal electrodes in liquid hydrocarbons produce nanocomposite materials, i.e. metal nanoparticles embedded in a hydrogenated C-matrix [7]. The C-matrix limits the diffusion of ambient air into nanoparticles and, therefore, inhibits their oxidation. Notably, the quality of the matrix, particularly the degree of graphitization, depends on the molecular composition of the hydrocarbon [7]. The latter pathway of nanomaterial synthesis (i.e. ion reduction) is based on the interaction between plasma species and the ions present in solution. These ions are supplied by precursors or by metal electrode dissolution, and they are reduced to atoms upon interacting with the plasma species. In turn, the atoms aggregate to form nanomaterials. CuO, Au, Ag... nanoparticles have been successfully synthesized using this approach [8-10].

Recently, we have proposed and studied a novel configuration of in-liquid discharges, that is discharges at / near the interface of two immiscible liquids [11]. In this communication, we present the experimental setup used to

produce such discharges between a liquid hydrocarbon and aqueous solutions of varying electrical conductivity (this property is varied by adding salts to distilled water). The investigated liquid systems include i) heptane/water, ii) heptane/(water + Ag nitrate), and iii) cyclohexane/(water + Ni-, Co-, and Fe-nitrate). The electrical and optical characteristics of discharges produced with different systems are presented, and the nanomaterials formed in each case are analyzed.

## 2. Experimental setup

The experimental setup is shown in Fig. 1. It consists of a quartz tube filled with an aqueous solution (distilled water with metal salts of varying nature and concentration) and a liquid hydrocarbon (heptane or cyclohexane). Since the two liquids are immiscible, a stable interface is obtained between them. The upper electrode is a carbon rod, and the distance between its sharp tip and the interface can be adjusted so that the tip is positioned in the aqueous solution ( $z < 0$ ), in the hydrocarbon liquid ( $z > 0$ ), or at the interface ( $z = 0$ ). The lower electrode is also a carbon rod; however, its tip is flat. The position of this electrode is fixed in the aqueous solution, far from the interface. A positive high voltage power supply is connected to the upper electrode, while the lower electrode is grounded.

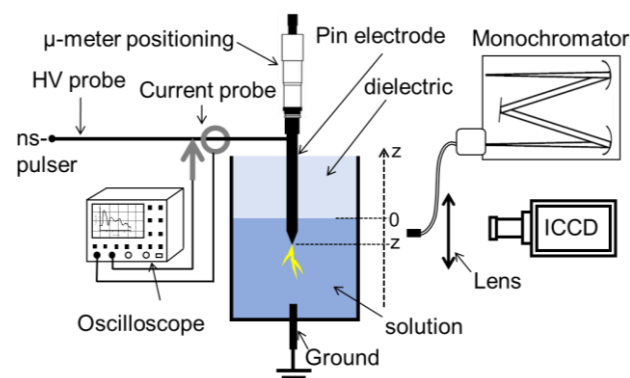


Fig. 1. Scheme of the experimental setup.

In this work, discharges were ignited at 22 kV voltage amplitude and 100–500 ns pulse width using a nanosecond positive pulsed generator. The discharge repetition rate was set to 1 Hz during imaging experiments and to 10 Hz

during synthesis for a period of 30 min. The electrical characteristics, voltage and current, of the discharge were measured using a high-voltage probe and a current coil, respectively, and they were visualized using an oscilloscope. An ICCD camera coupled with a delay generator was used to observe the plasma emission. Optical emission spectroscopy was also performed using an adapted spectrometer. Finally, the synthesized nanostructures were characterized using conventional techniques such as transmission electron microscopy (TEM), scanning electron microscopy (SEM), UV–vis absorption spectroscopy, and Fourier transform infrared spectrometry (FTIR).

### 3. Results and discussion

#### 3.1. Optical and electrical characterization

Fig. 2 shows 1.5- $\mu$ s-integrated images of the discharge emission observed under various conditions of  $z$  and electrical conductivity ( $\sigma$ );  $\sigma$  was adjusted by adding KCl. In the heptane/water ( $\sigma = 10 \mu\text{S/cm}$ ) system, a filamentary emission with relatively short filaments ( $\sim 0.5$  mm) is obtained when the pin is in distilled water, far from the interface. As the tip approaches the interface, the number, intensity, and length of the plasma filaments increase. The filaments observed at the interface ( $z = 0$ ) are even longer than those detected in water, and they propagate horizontally instead of towards the cathode. This means that when  $z = 0$ , the plasma emission is influenced by the interface. The horizontal propagation of filaments may be attributed to the refraction of the E-field lines traversing the interface, which in turn is due to the discontinuity of dielectric permittivity [12, 13]. At  $z > 0$ , i.e. when the pin is in heptane, no discharges are produced in the liquid system. The plasma emission observed in the heptane/(water + KCl) system at  $\sigma = 100 \mu\text{S/cm}$  is similar to that detected in the heptane/distilled water system; however, the intensity of filaments is lower. In this system, discharges may be generated in heptane, at distances near zero.

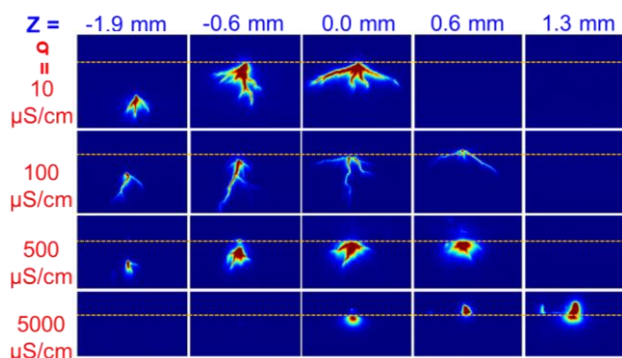


Fig. 2. 1.5- $\mu$ s-integrated images showing the plasma emissions produced in heptane/water under different conditions of  $\sigma$  and  $z$ . The discontinuous line represents the interface.

When  $\sigma$  is increased to  $500 \mu\text{S/cm}$ , the filamentation phenomenon is significantly suppressed, with fewer, shorter, wider, and more intense filaments observed at ( $z = 0$ ) or near the interface, on the side of water ( $z < 0$ ). A localized emission with short elliptical-like filaments is also observed in heptane at  $z = 0.6$  mm; however, no emission is detected at  $z = 1.3$  mm. Finally, at  $5000 \mu\text{S/cm}$ , filamentation is totally suppressed, and a single plasma emission zone is observed only at  $z \geq 0$ . The emission is elliptical-like when  $z = 0$ , and it is concentrated in a single wide channel ( $\sim 1$ -mm-diameter) when the electrode tip is in heptane.

The acquired optical emission spectra (Fig. 3) of discharges occurred at the interface of heptane/(water + KCl) demonstrate that the two liquids are dissociated, as evidenced by the detection of  $\text{H}\alpha$ , O, and  $\text{C}_2$  Swan bands, in addition to a continuum component. Notably, the  $\text{H}\alpha$  line detected at  $5000 \mu\text{S/cm}$  is much broader than that recorded at  $100 \mu\text{S/cm}$ , indicating a higher electron density at the former condition ( $\sim 1 \times 10^{19}$  vs.  $3 \times 10^{18} \text{ cm}^{-3}$ ).

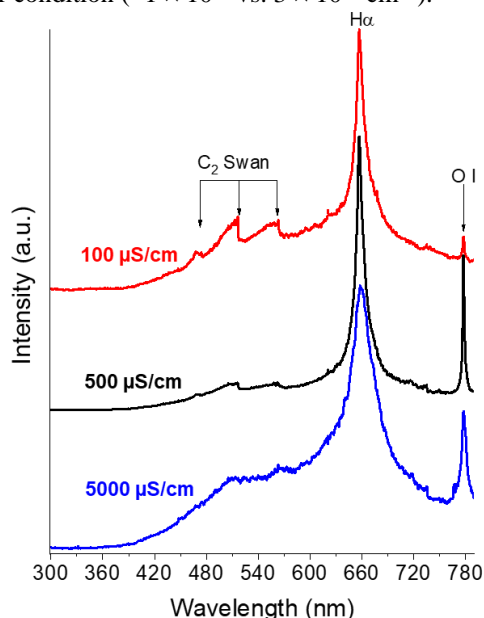


Fig. 3. Optical emission spectra of discharges in different heptane/water systems at  $z = 0$  and variable  $\sigma$ .

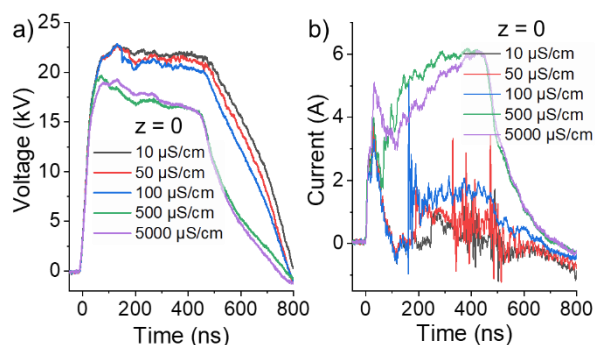


Fig. 4. a) Voltage and b) current waveforms of typical discharges in heptane/(water + KCl) at  $z = 0$  and variable  $\sigma$ .

The electrical characteristics also show a dependence on  $\sigma$ . As shown in Fig. 4a, the voltage waveforms recorded at  $z = 0$  (pin at the interface) and  $\sigma \leq 100 \mu\text{S}/\text{cm}$  exhibit perturbation, and a drop of a few kilovolts is observed at higher  $\sigma$ . Meanwhile, the current waveforms measured at  $z = 0$  present a series of current peaks, with values in the order of a few amperes in the case of  $\sigma \leq 100 \mu\text{S}/\text{cm}$ . At higher  $\sigma$ , a continuous increase in current is observed during the pulse, and the current intensity is relatively higher than that detected at lower  $\sigma$ .

In summary, the optical and electrical characteristics of discharges at / near the interface of two immiscible liquids depend on the experimental conditions, particularly the electrical conductivity of the aqueous solution and the pin position regarding the interface. Moreover, as evidenced by current measurement and optical emission, the discharge mode changes from streamer-like to spark-like at  $\sigma > \sim 500 \mu\text{S}/\text{cm}$ .

### 3.2. Nanomaterial characterization

In this section, we identify the nanomaterials produced by discharges at / near the interface of heptane/water, heptane (water + Ag nitrate), and cyclohexane/(water + Ni-, Co-, and Fe-nitrate).

*(i) Discharges at the heptane/water interface.* The discharges produced at the interface of heptane and water exhibit a horizontally propagating streamer-like emission. One expects that the discharge will dissociate both liquids, resulting in the generation of many reactive species, such as C, O, H, and  $\text{C}_2$ . These species recombine to produce nanomaterials. During plasma processing, changes in the colors of both liquids, as well as the formation of gel-like material at the interface are visually discerned. Indeed, when the cell is kept at rest for a certain period, both liquids become clear, and an opaque, gel-like substance is formed.

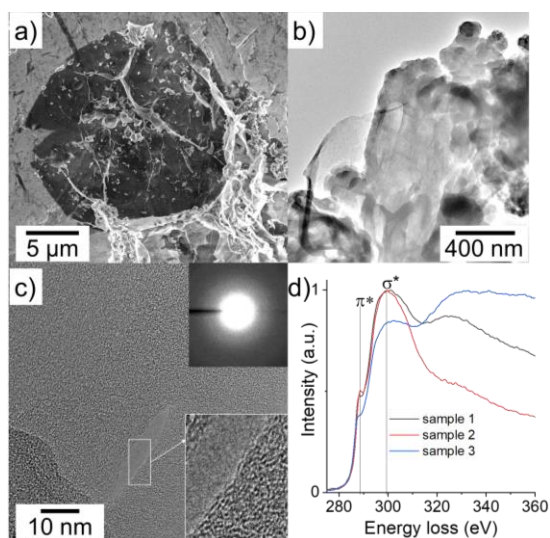


Fig. 5. A) SEM image of the material produced by discharge at the heptane/water interface. B) Low- and C) high-resolution TEM images of the material. D) EELS spectra of different samples.

SEM analysis of the produced material after extraction and evaporation on an Al substrate (Fig. 5a) shows a continuous film-like deposited on the substrate. Low- and high-resolution TEM images (Figs. 5b and 5c, respectively) of this film reveal that it is amorphous; however, some zones with crystalline structure are also observed (encircled zone). The EELS spectra of three analyzed samples (Fig. 5d) are consistent with typical amorphous structure. However, the inconsistency between the spectra indicates that the film is not homogeneous, which further supports its varying crystalline nature. Interestingly, the film is transformed into a nanoneedle-like material after heating at  $500^\circ\text{C}$  for 2h. The TEM image shown in Fig. 6 and the corresponding SAED pattern (inset) demonstrate that the needles have a crystalline structure. Furthermore, their diffraction pattern corresponds to that of graphene. Therefore, we believe that the heating process eliminates the ‘unstable components’, and only the stable one remains.

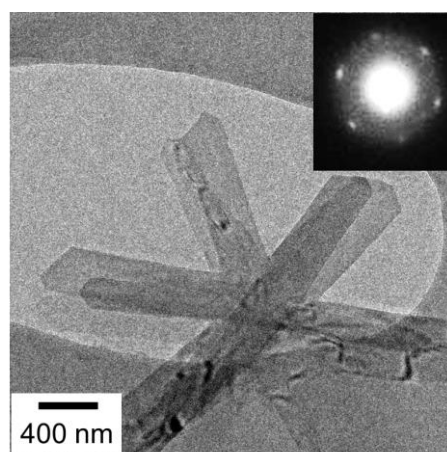


Fig. 6. TEM image of nanomaterial produced by discharge at the heptane/water interface after heating at  $500^\circ\text{C}$  for 2h.

*(ii) Discharges at the heptane/(water + Ag nitrate) interface.* The discharges produced using this configuration are spark-like, and they dissociate both liquids to produce many reactive species (C, O, H,  $\text{C}_2$ , etc.). Figs. 7a and 7b present typical TEM images of the material formed in heptane and in solution, respectively, after discharge. Clearly, the material collected from heptane is composite-like, i.e. Ag nanoparticles embedded in C-matrix, while that collected from the solution is matrix free. Moreover, the size of particles formed in solution is much larger ( $\sim 10\times$ ) than that of particles formed in heptane.

These results suggest two mechanisms of synthesis, both of which are based on the reduction of Ag ions ( $\text{Ag}^+$ ) by plasma species to form  $\text{Ag}^0$ . The main reactions reported in similar systems are  $\text{Ag}^+ + e \rightarrow \text{Ag}^0$  and  $\text{Ag}^+ + \text{H} \rightarrow \text{Ag}^0 + \text{H}^+$  [14]. In heptane, it seems that the presence of C-species leads to the formation of a carbon shell around the particles, which stops the aggregation and leads to smaller particles. However, in solution, the particles continue to

grow due to the lack of a matrix, and sizes as large as 200 nm are observed.

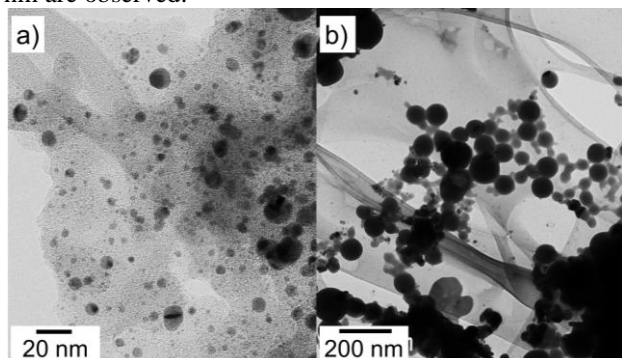


Fig. 7. TEM images of nanoparticles produced by discharges in heptane/(water + Ag nitrate); samples collected from a) heptane and b) aqueous solution.

**(iii) Discharges at the cyclohexane/(water + Ni-, Co-, and Fe-nitrate) interface.** This configuration is very similar to the previous one, except that three metal salts are added to water instead of one. Ideally, nanoalloys would be formed using this liquid system. TEM analysis of the nanomaterial formed in cyclohexane (Fig. 8a) shows nanoparticles embedded in a C-matrix. A high-resolution image of a typical particle (inset of the image) reveals that it has crystalline structure, with an interplanar distance of  $\sim 0.20$  nm. This distance is very close to that of Ni (111), Co (111), and Fe (111). Moreover, the EDS spectrum (performed on Fig. 8a) presented in Fig. 8b confirms the presence of Fe, Co, and Ni elements in the analyzed sample, in addition to C. The three elements are also detected in the EDS spectra of single nanoparticles, which indicates that they consist of FeNiCo nanoalloys. In fact, other binary mixtures were also tested, namely Ni- + Fe-nitrate, Ni- + Co- nitrate, and Fe- + Co-nitrate, and the obtained results demonstrate that NiFe, NiCo, and FeCo nanoalloys are produced, respectively.

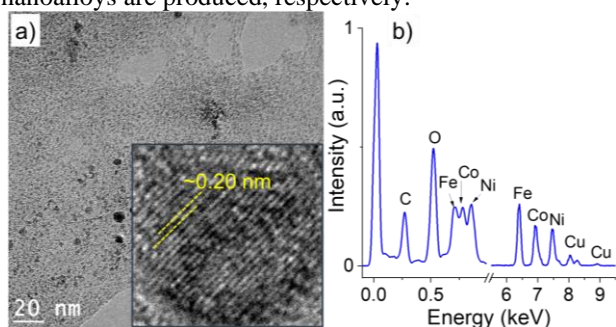


Fig. 8. a) TEM image of nanoparticles produced by discharges in cyclohexane/(water + Ni-Fe-Co nitrates). b) EDS spectrum acquired on a).

#### 4. Conclusion

In summary, the growing research field of discharge in liquid has shown great potential in many fields, particularly the synthesis of nanomaterials. These materials are produced via two main pathways: electrode erosion and ion reduction. Both pathways induce liquid dissociation, and

they can occur individually or together, depending on the discharge conditions, particularly the electrical conductivity of the liquid. In this communication, we perform electrical and optical characterization of discharges at / near the interface of two immiscible liquids. The nanomaterials produced using this novel technique are also characterized. The obtained results show that the discharge properties are strongly dependent on the electrode position relative to the interface, as well as the electrical conductivity of the liquid. Discharges at the heptane/water interface produce carbonaceous film-like material, whereas discharges at the interface of heptane/(water + Ag nitrate) lead to nanocomposites (Ag nanoparticles embedded in C-matrix) in heptane and large particles in aqueous solution. When multiple metal salts are added to the solution, binary and ternary nanoalloys are produced. Finally, we are convinced that this type of discharge can be used to synthesize novel nanomaterial with novel properties.

#### 5. Acknowledgements

This research was funded by the Natural Sciences and Engineering Research Council of Canada (NSERC). The authors thank the Fonds de Recherche du Québec—Nature et Technologie (FRQ-NT) and the Canada Foundation for Innovation (CFI) for funding the research infrastructure.

#### 6. References

- [1] T. Belmonte et al., Journal of Physics D: Applied Physics, 47(22), 224016 (2014).
- [2] Q. Chen et al. High Voltage, 7(3), 405-419 (2022).
- [3] P. Bruggeman et al. Plasma sources science and technology, 25(5), 053002 (2016).
- [4] D. Mariotti et al. Plasma Processes and Polymers, 9(11 - 12), 1074-1085 (2012)
- [5] A. Hamdan et al. Plasma Chemistry and Plasma Processing, 41, 433-445 (2021).
- [6] T. Merciris et al. Journal of Applied Physics, 129(6), 063303 (2021).
- [7] X. Glad et al. Scientific reports, 11(1), 1-12 (2021).
- [8] C. Richmonds et al. Appl. Phys. Lett., 93(13), 131501 (2008).
- [9] T. Velusamy et al. Plasma Processes Polym., 14(7), 1600224 (2017).
- [10] J. Patel et al., 24(24), 245604 (2013).
- [11] A. Hamdan et al., AIP Advances, 6(10), 105112 (2016).
- [12] A. Hamdan et al., Plasma Sources Science and Technology, 30(5), 055021 (2021).
- [13] N. Babaeva et al. Journal of Physics D: Applied Physics, 42(13), 132003 (2009).
- [14] V. Kondeti et al. J. Vac. Sci. Technol., A,35(6), 061302 (2017).